Journal of Structural Geology 30 (2008) 1254–1263

Contents lists available at ScienceDirect

Journal of Structural Geology

journal homepage: www.elsevier.com/locate/jsg

Growth of the volcano-flank Koa'e fault system, Hawaii

Dean M.W. Podolsky, Gerald P. Roberts*

The Research School of Earth Sciences, Birkbeck and University College, University of London, Gower Street, London. WC1E 6BT, UK

ARTICLE INFO

Article history:
Received 8 May 2007
Received in revised form 20 May 2008
Accepted 11 June 2008
Available online 21 August 2008

Keywords:
Koa'e fault system
Volcano flank
Normal faults
Propagation
Monoclines
Lava re-surfacing

ABSTRACT

Structural mapping of the Koa'e fault system, located on the south flank of Kilauea Volcano, Hawaii, has been carried out to study the relationship between fault propagation and re-surfacing by lava flows. The 1.9-km long White Rabbit Fault faces uphill towards the summit of the Kilauea, and has produced c. 8 m vertical offset of a young lava flow (500–750 years). The fault exhibits multiple peaks in its throw-distance profile, suggesting recent linkage between at least 2 separate faults at the surface. However, the width of a monocline associated with the fault shows a single maximum of c. 40 m, located near the centre of the overall fault trace. We suggest monocline width is related to heave across the fault at depth (a minimum of c. 40 m) beneath the most recent lava that re-surfaced the fault. The surface monocline records re-emergence of a fault that had previously propagated to the surface prior to recent lava deposition rather than upward propagation of a new fault. Overall, the fault displays a growth geometry with displacements increasing with depth. The above implies that the Koa'e faults pre-date the lavas exposed at the surface on the volcano flank, and are a long-lived feature of the volcano dynamics, despite the small offsets across the faults at the surface.

1. Introduction

The flanks of active volcanoes can become deformed by growing normal faults, and these faults can become covered by lava flows (e.g. Parfitt and Peacock, 2001; Peacock and Parfitt, 2002; Day et al., 2005; Holland et al., 2006). Such lava–fault relationships produce growth faults that influence the stability of the volcanic edifice because the relative rates of faulting and lava deposition can either steepen or shallow slopes on the volcano flank. Thus, interest is growing regarding the geometrical evolution of such faults, the rates of lava deposition relative to rates of vertical offset across faults, and the longevity of faulting relative to the age of the volcano as a whole (Day et al., 2005; Martel and Langley, 2006).

In particular, re-surfacing of pre-existing faults by lavas will complicate attempts to infer fault propagation histories. The growth fault geometry of a fault that ponds lava will be associated with relatively small values for displacement at the surface, because here displacement will only have developed since the last lava re-surfacing event. At times, no throw will be present at the surface if the fault has not ruptured to the surface since the flow of lava. At greater depths, the growth fault geometry will be characterized by displacements that increase downwards into successively older volcanic layers. Reactivation of the fault at depth will cause propagation of the fault up through the un-faulted lava at the surface, but this upward propagation will only occur from depths of a few metres. This process will obscure the signal of longer-term fault growth from greater depths. Thus, in order to study how faults affect volcano evolution during fault propagation, lava–fault relationships must be understood.

An example of such growth faults are those within the Koa'e fault system, Hawaii, that face north towards the summit of Kilauea Volcano and are known to have (1) ruptured at the surface and grown in historical earthquakes, and (2) diverted/ponded recent lava flows (Swanson et al., 1976; Day et al., 2005; Fig. 1). The faults are associated with vertical offsets of lava surfaces of only a few metres to tens of metres. Uncertainty exists concerning how these active faults propagate, and their age relative to the volcano, given that they have a very subdued topographic expression compared with the Hilina fault system that faces south away from the summit of Kilauea Volcano (vertical offsets of lavas of tens to hundreds of metres; Fig. 1). The age of the Koa'e fault system has been suggested to be as little as 1000 years old (Duffield, 1975; Swanson et al., 1976; see Day et al., 2005), mainly due to their subdued topographic expression, whilst more recent studies suggest the faults may be older, with the subdued topographic expression due to recent covering by lava (e.g. Day et al., 2005). Regarding fault propagation, debate exists as to whether such faults propagate upwards from depth towards the surface (Martel and Langley, 2006, Holland et al., 2006; Kaven and Martel, 2007; see also Grant and Kattenhorn, 2004 for an example from Iceland), or downward from the surface (McGill and Stromquist, 1975, 1979; Stromquist, 1976; Cartwright et al., 1995; Cartwright and Mansfield, 1998). Detailed structural

* Corresponding author.
E-mail address: gerald.roberts@ucl.ac.uk (G.P. Roberts).

0191-8141/$ – see front matter © 2008 Elsevier Ltd. All rights reserved.
doi:10.1016/j.jsg.2008.06.006

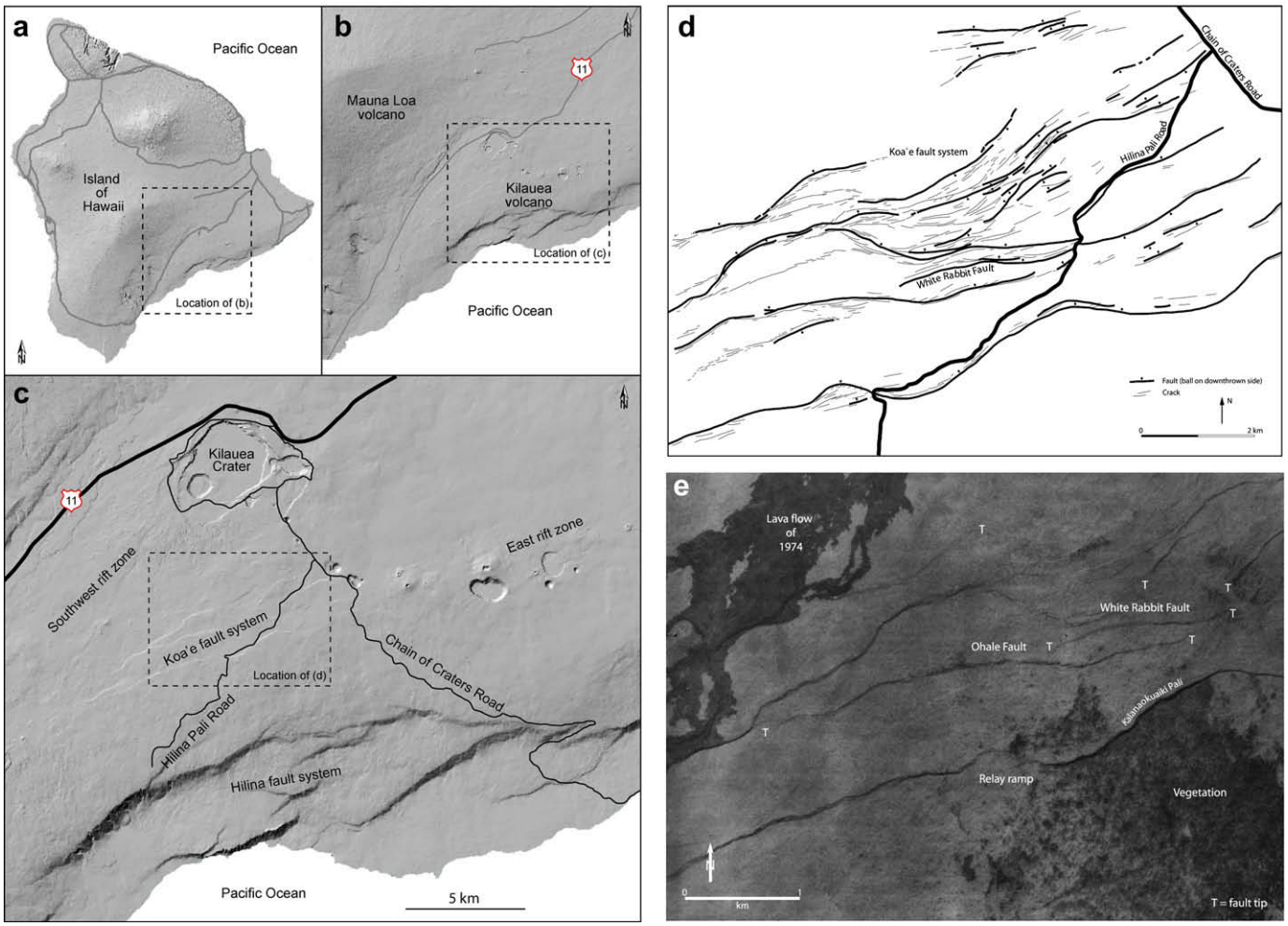

Fig. 1. (a) Map of Island of Hawaii, based on SRTM digital elevation model (DEM), showing the field study area. (b) Location of Koa'e fault system in relation to Kilauea Volcano, Hawaii. (c) Detail of the south flank of Kilauea Volcano, Hawaii, showing the summit of Kilauea and location of the Koa'e fault system. (d) Generalized structural map of Koa'e fault system showing major regional faults and cracks. It can be seen that a majority of the faults are north-facing. (Map redrawn from the Geologic Map of the Summit Region of Kilauea Volcano, Hawaii, Neal and Lockwood, 2003.) (e) Aerial photograph (USGS 1:24,000) of the Koa'e fault system. The White Rabbit Fault is located in the upper right of the image. The fault appears as a double line; this double line includes the trace of the monocline in the hangingwall (on the north side of fault trace). The fault trace appears as a dark line due to the shadow cast by the footwall scarp onto the monocline. Areas of vegetation, the largest of which is located in the lower right of the photo, can be seen throughout the area. In the top left, lava flows from 1974 are visible; notice the diversion of the flow caused by the north-facing faults.

mapping and modelling of the Koa'e faults, and in particular monoclines related to faulting, suggest that the faults propagated upwards from depths of few hundred metres *during* evolution of the faulted monoclines observed at the surface (Martel and Langley, 2006; Holland et al., 2006; Kaven and Martel, 2007). Upward propagation of faults from depths of several hundred metres is modelled within a "linear elastic, isotropic, isothermal, homogenous, semi-infinite continuum". However, we suggest that differentiation of upward versus downward propagation may be complicated by growth fault geometries. This is because (a) surface displacements may not characterize those at depth due to growth faulting (see above), (b) the material will not be homogenous and isotropic because un-faulted lavas will overlie faulted lavas that are mechanically decoupled across faults, and most importantly (c) the monoclines observed at the surface will record upward propagation *since* deposition of the last lava, but will not record propagation from depths of hundreds of metres over longer timescales. Whether such small-scale upward propagation typified earlier faulting cannot be interpreted from observations of surface lavas as they had not formed during earlier fault growth.

The goal of this paper is to develop a fault-evolution model that constrains the growth history of faults in the Koa'e fault system that are known to pond and divert lava flows. The Koa'e fault system was selected because of the excellent exposure of features, including extensive faults and monoclinal structures. In particular, we have conducted detailed mapping of the White Rabbit Fault which forms part of the Koa'e fault system. We emphasize what can be learned from comparison of throw-distance profiles for the fault and maps of the width of monoclines produced by fault propagation. The fault in question shows evidence of having been a single fault that was re-surfaced by lava. Ongoing slip has allowed upward propagation of the single fault from depth in the form of at least two fault segments. The upper portions of these fault segments only linked along strike after reaching the surface. We use these findings to discuss the evolution of faulting on the flank of Kilauea Volcano, relative rates of vertical fault offset and lava deposition, the longevity of faulting and volcano edifice stability.

2. Geological setting

The Koa'e fault system is a zone of normal faulting located on the south flank of Kilauea Volcano, Hawaii (Figs. 1 and 2), an active basaltic shield volcano. Kilauea Volcano is built on the southeast flank of Mauna Loa Volcano, and is the southeastern most shield

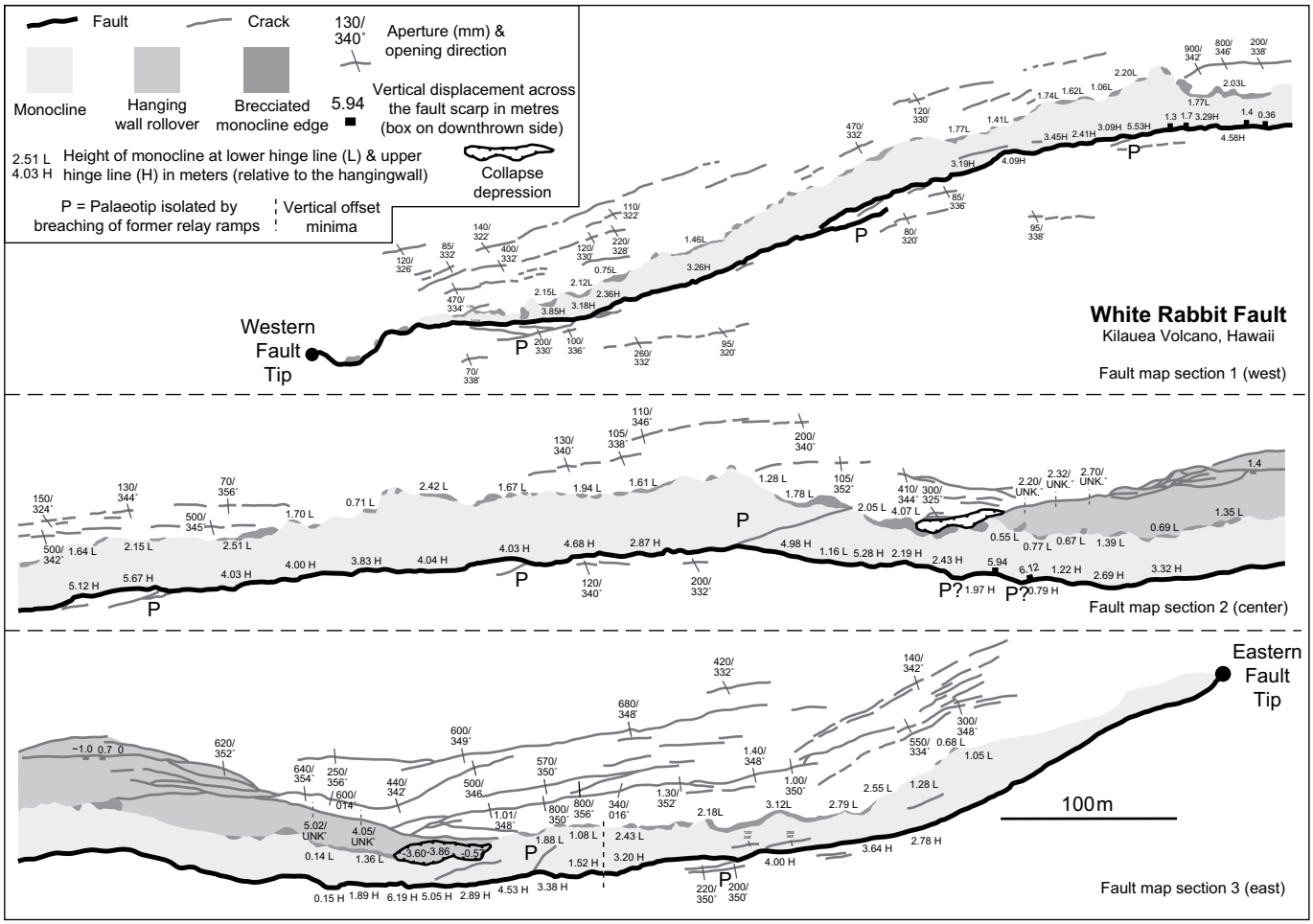

Fig. 2. Detailed structural map of the White Rabbit Fault.

volcano in the Hawaiian-Emperor chain of islands in the Pacific Ocean (Clague and Dalrymple, 1987; Swanson et al., 1976).

The Koa'e fault system trends east-northeast and is located just south of the summit caldera. The zone of faulting is about 12 km long and the width tapers westward from 3 km to 1 km (Duffield, 1975). It is characterized by sinuous fault traces composed of en-echelon faults and north-facing fault scarps. The fault system merges at its two ends with the Southwest and East Rift Zones (Fig. 1b), and together form a continuous fault zone of extension that separates the structural block of the south flank from the rest of the volcano (Duffield, 1975).

The location of the Koa'e fault system on Kilauea Volcano, and specifically within the Kau Desert, is illustrated in Fig. 1c. The Koa'e fault system contains many faults and monoclines (Fig. 1d). The faults can be seen quite clearly on 1:24,000 scale aerial photographs (Fig. 1e). From the ground, the faults are quite prominent as topographic scarps (Fig. 2), which are known to grow in historical earthquakes (Figs. 3–6).

The topography offset by the scarps is irregular and most of the area is surfaced by pāhoehoe lava from the Kalue flow (Holcomb, 1987). This flow has been dated using radiocarbon and palaeomagnetic methods which have indicated an age of 500–750 years (Holcomb, 1987): the scarps show where the Koa'e fault system offsets this young lava. Also, in 1974 a lava flow from Kilauea flowed down the volcano flank and was diverted by the topographic scarps on the Koa'e faults.

The origin of the Koa'e fault system is believed to be closely related to intrusion of magma into the two rifts, principally the east rift zone. These intrusions are accompanied by earthquake swarms and harmonic tremor. The Koa'e fault system is likely to be the result of the culmination of multiple seismic episodes. Kinoshita (1967) described four events that occurred during the period from 1938 to 1965. Each event was documented to have produced ground cracking and deformation near the study area. Kinoshita provided an estimate of the number of earthquakes linked to each event. The total number of earthquakes recorded during these events are 88 in 1938, 656 in 1950, 3000 in 1963, and >10,000 in 1965. Kinoshita pointed out that the number of earthquakes that occurred in the early events (1938 and 1950) is likely to be an under-estimate because the type of mechanical seismograph being used at the time was not capable of identifying all events. The deformation typically included ground cracking in the eastern part of the Koa'e fault zone, but two events, 1963 and 1965, occurred near the study area; the event in 1965 is especially noteworthy because it shows that the faults grow in earthquakes.

On December 24, 1965, an eruption occurred along the east rift zone of Kilauea. An eruptive fissure opened in an en echelon zone about 2 miles long and formed a 47 foot deep lava lake in a nearby crater (Fiske and Koyanagi, 1968). The eruption marked the beginning of a major seismic episode that lasted for more than a week during which thousands of earthquakes were recorded whose epicentres occurred in a narrow area extending from the upper east rift zone westward (see Fig. 1b) along the Koa'e fault zone (Fiske and Koyanagi, 1968). Hundreds of cracks with a combination of right-lateral offset and vertical displacement opened up in this area; one of these cracks is worthy of specific mention. At 08:15 on

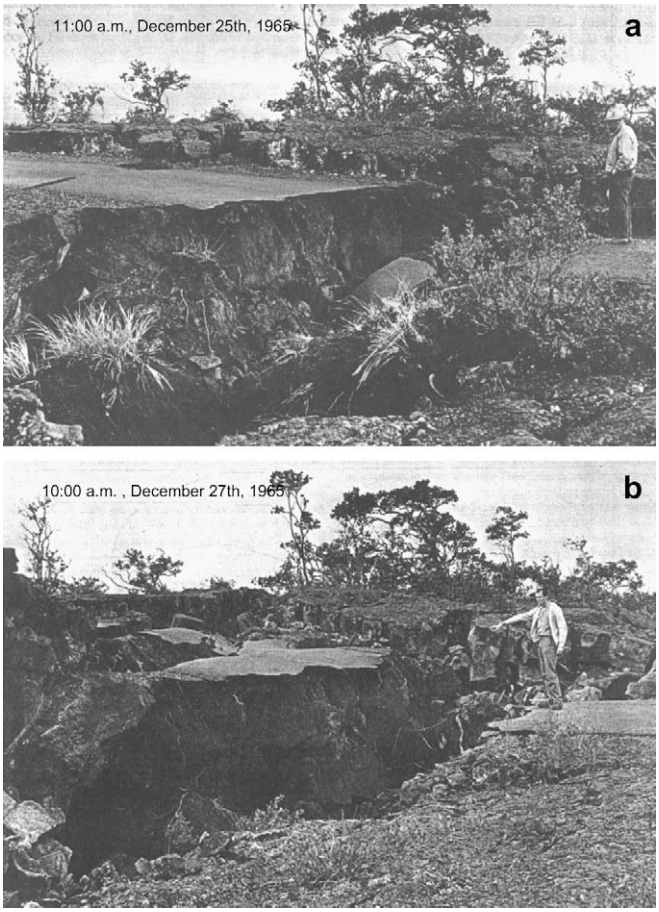

Fig. 3. (a) Photo of damage caused by earthquake swarm resulting from fissure eruption along Kalanaokuaiki Pali at Hilina Pali Road, Kilauea Volcano, Hawaii. Slumping of edges has caused initial 3 foot crack to enlarge to about 8 feet, as seen in front of person. Photo taken at 11:00 on December 25th, 1965 and reproduced from Fiske and Koyanagi, 1968. (b) Subsequent photo taken at 10:00 on December 27th at same location showing the main gap in the road enlarged to a width of about 10 feet. Additional damage has been caused by continuation of seismic swarm and an earthquake which was witnessed to have nearly toppled a nearby vehicle. Vertical displacement totals about 3 or 4 feet. Photo reproduced from Fiske and Koyanagi (1968).

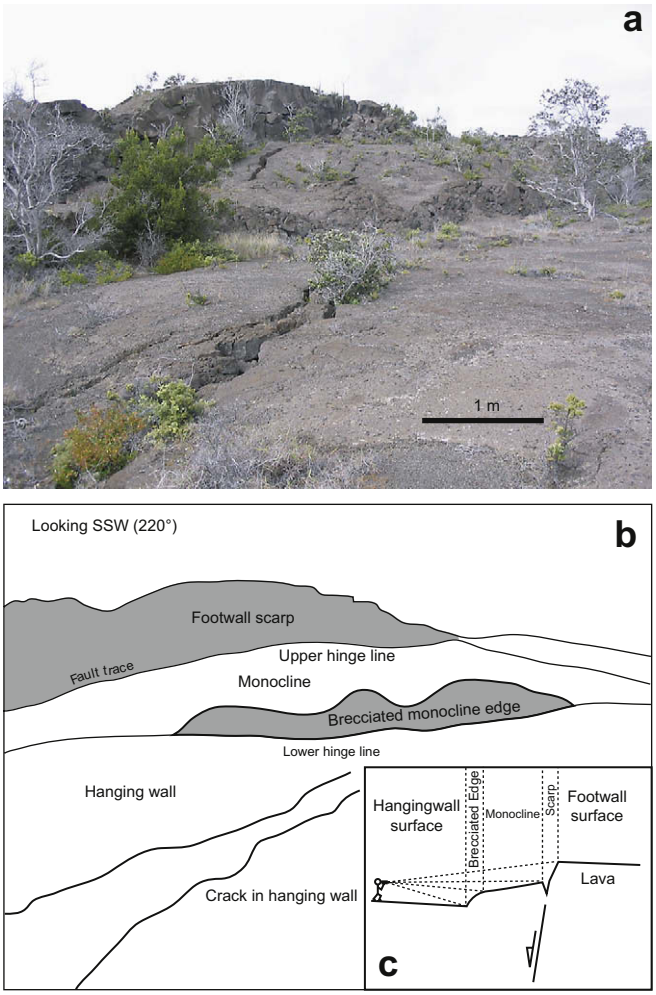

Fig. 4. (a) View of monocline along strike of White Rabbit Fault showing gentle curve from the upper hinge line (at base of scarp) to lower hinge line (centre of photograph). Note brecciated ridge along lower hinge line. (b) Interpretation of the photograph shown in Fig. 4a. The gentle curve of the upper hinge line to the lower hinge line can be seen in the centre of the diagram. (c) Cartoon showing how vertical offsets were measured by combining the vertical dimensions of the structures relative to the hangingwall surface.

December 25, 1965, a crack along the Hilina Pali Road at Kalanaokaiki Pali was observed (Fig. 3, located in Fig. 1d). It was barely 2 feet wide at this time. At 08:40, "the area was wrenched by an earthquake so violent that it nearly toppled a vehicle parked nearby" (Fiske and Koyanagi, 1968). This earthquake caused the crack to open to about 5 feet wide. This crack and others in the immediate area continued to widen as the earthquake swarm continued until December 27, 1965 when the main crack had opened to its full extent (Fiske and Koyanagi, 1968). The total vertical offset of this crack was about 1.0–1.2 m. Fig. 3 is a reproduction of a two photographs published by Fiske and Koyanagi in their paper from 1968. Fig. 3a shows the crack at 11:00 on December 25th when the Hilina Pali Road was crossed by one crack about 80 cm wide. The photo in Fig. 3b was taken at 10:00 on December 27th when the main crack had opened to a width of about 3–4 m and new cracks had formed as a result of continued earthquakes. The above shows that offsets across the faults we study accumulate during earthquakes.

The potential for renewed dilation and faulting occurs whenever magma is forcefully injected into the rift zones as steeply dipping dikes. The initial depth of intrusion is poorly known, but seismic evidence suggests 2-5 km (Duffield, 1975). Koyanagi et al. (1972) suggest that the fault zone of extension may penetrate to a depth of about 10 km, the approximate level of the ocean floor, thereby detaching the south flank from the rest of the volcano (Duffield, 1975). Duffield (1975) applies Hansen's (1965) "graben rule" to calculate a depth of 667 m, but this is based on the assumption that the entire fault zone is one complex graben. Parfitt and Peacock (2001) suggest that the Koa'e fault system is probably underlain by two or three faults, the largest of these being at least ~14 km long extending to a depth of at least ~4 km and possibly to the depth of the basal thrust (~9–10 km).

3. The White Rabbit Fault

The previously unnamed White Rabbit Fault (Swanson, personal communication, 2004) has been mapped in detail. Faults at the surface of the Koa'e fault system are all vertical to near-vertical, with throw and opening displacements, and no evidence of contact across the fault at the surface. The tectonic cracks and faults of the system exploit cooling joints in the basaltic lava resulting in highly serrate boundaries. These boundaries enable the opening direction and amount of horizontal offset to be determined because the opposing walls can be almost perfectly matched like the

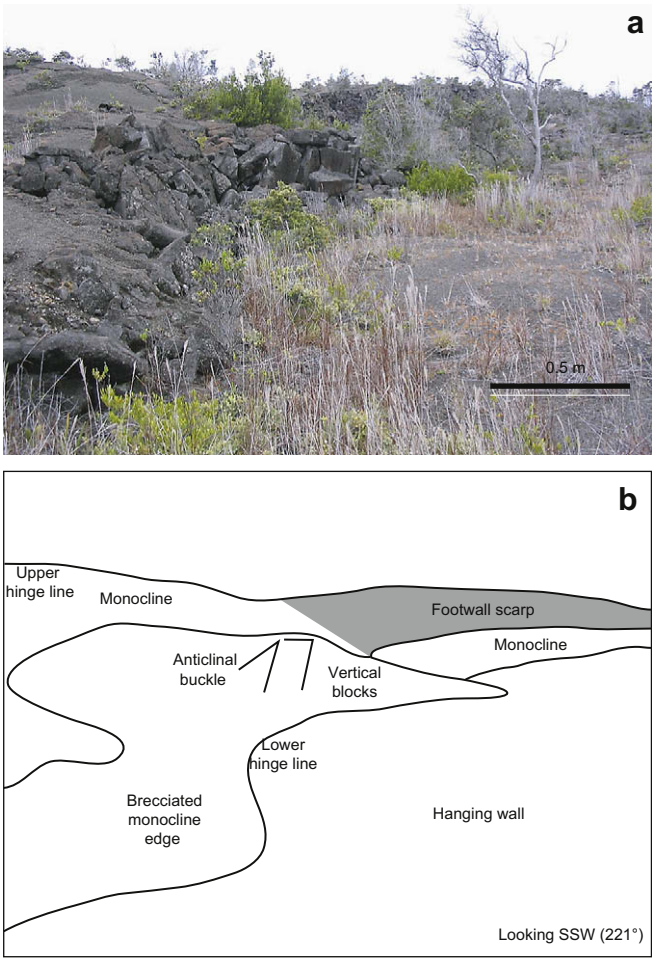

Fig. 5. (a) Photo of monocline taken along strike of the White Rabbit Fault showing abrupt, elevated ridge along the lower hinge line with near-vertical blocks and a brecciated ridge. (b) Interpretation of the photograph shown in Fig. 5a. Near the centre of the diagram are two examples of anticlinal buckles and vertically tilted blocks found along the fault. The north-facing fault scarp and continuation of the monocline, both hidden by vegetation in the photograph, are delineated here for easier identification.

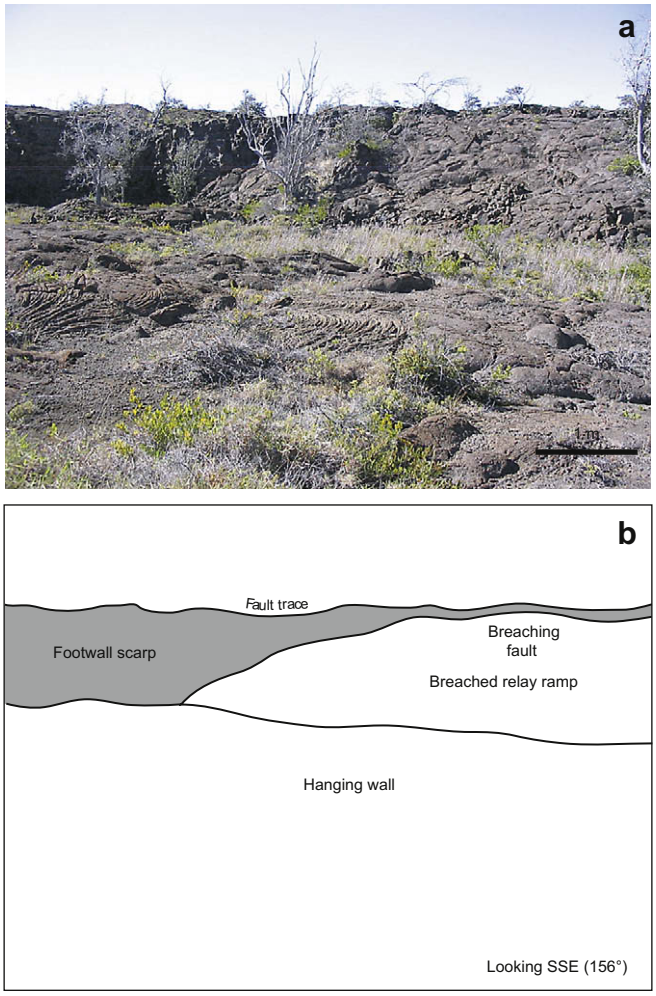

Fig. 6. (a) Photograph of a breached relay ramp along strike of the nearby Ohale Fault. The fault scarp can be seen on the left of the photograph, while on the right of the photo the relay ramp, breached by the fault at the top of the ramp. In the foreground, the topography can be seen to vary due to the form that the lava takes when cooled. (b) Interpretation of the photograph shown in (a). The breaching fault shown at the top of the relay ramp has developed <1 m of throw, while to the left the throw is nearly 6 m.

pieces of a jigsaw puzzle (Duffield, 1975; Peacock and Parfitt, 2002; Martel and Langley, 2006). However, where crack opening involves collapse of the crack walls, no opening directions can be measured.

Monoclines are another characteristic feature of the White Rabbit Fault and the Koa'e fault system in general, and parallel the length of faults in the hanging wall. They are curved in map view and follow the traces of the faults. The monoclines vary in height and width along strike of the fault. The monocline hinge zones either curve gently into the hanging wall (Fig. 4a) or end abruptly at elevated, often brecciated ridges (labelled brecciated monocline edge, Fig. 4b) (see Macdonald, 1957).

Numerous relay ramps are present along strike of the White Rabbit Fault. Most of these ramps are still coherent, as seen in Fig. 5, but others have been reduced to blocks of rubble at the base of the footwall scarp. The relay ramps can be divided into two types: breached, and un-breached (see Fig. 7).

It is evident that these ramps, monoclines and scarps have been known about for many years (Macdonald, 1957). However, prior to our work, the relationship between monocline width and fault offset had not been mapped in detail; this work forms the focus of this paper.

4. Field method and logistics

The White Rabbit Fault was chosen for mapping because preservation of the fault trace, fault plane, cracks, and monocline is exceptionally good due to the lack of substantial sedimentary/pyroclastic deposits and vegetation in the region.

Detailed structural mapping in the field was carried out on USGS topographic maps and un-rectified aerial photographs with a scale of 1:12,000 which form part of an aerial survey of the island of Hawaii in January 1992. Mapping of the main scarp and monocline involved the measurement of total vertical offset (throw), opening direction, monocline width, and the total length of the fault. These measurements were made using a handheld GPS, a laser rangefinder that could also constrain relative elevations through electronic tilt measurements (Fig. 4c), a compass and clinometer, and tape measures. Laser measurements of the vertical dimensions of monoclines and scarps were taken from distances less than 15 m from the front edge of the monocline. Cracks in the hanging wall were mapped and the amount of opening and the opening direction were recorded at many points along the length of the fault. The mapping of these cracks was limited to within 15 m of the fault trace, in both the hanging wall and footwall. By combining

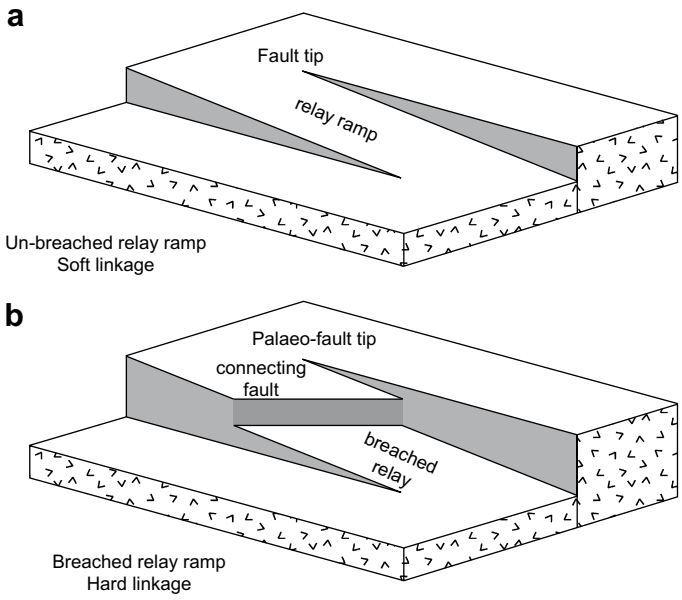

Fig. 7. Diagram of (a) un-breached relay ramp; and (b) breached relay ramp.

waypoints from GPS with identification of features on the aerial photographs on the ground, the maximum error in any of the fault trace length measurements and monocline widths is estimated to be no more than c. 2%; values for scarp height and monocline width are estimated to be in error by less than c. 3%.

5. Results

The White Rabbit Fault is approximately 1.9 km long and was mapped in its entirety, from tip to tip (Figs. 2 and 8). Overall, the fault can be divided into a number of segments separated by breached and unbreached relay zones. Lava surfaces in relay ramps dip at angles of 30–40° along the strike of the overall fault trace for distances of a few tens of metres. Where relay ramps are breached, the through-going fault has isolated remnant faults in the footwall or hangingwall (Fig. 2). We interpret these as the now-abandoned original lateral tips to the precursor soft-linked fault segments (palaeo-tips, e.g. McLeod et al., 2000).

Between relay ramps, the faults form topographic steps on the lava surface, comprising monoclinal flexures that are cut by fault scarps. Vertical offsets across the scarps are in the order of a few metres, but the total vertical offset of the lava surface is greater due to the presence of monoclines mentioned above. The fault scarps are almost vertical, because they involve some opening parallel to the ground surface, by amounts of up to a few metres. Opening directions range from 328 to 354°, defining an opening direction that is almost perpendicular to the fault trace (Figs. 2 and 8b). In places, fault scarps also exhibit dip-slip motion of up to c. 6 m. The monoclines, which achieve vertical relief of up to 6 m, parallel the fault trace for nearly its entire length. The steep limbs of the monoclines dip to the north at angles of approximately 30° (±10°), and extend into the hangingwall from the fault scarps for distances of up to almost 45 m. In most places along the monoclines, extensional fractures can be found which parallel the fault trace. These are near vertical, and have opening amounts ranging from a few centimetres to decimetres. In places, these fractures exploit cooling joints in the lava. On the edges of the monoclines opposite the scarps exist so-called "anticlinal buckles", first described by Macdonald (1957) and elaborated on by others (Martel and Langley, 2006; Kaven and Martel, 2007). These anticlinal buckles take the form of an elevated, and in places brecciated edge to the monoclines. Such anticlinal buckles are less than 2 m high and can extend along strike of the monoclines for tens of metres. In the central portion of the fault a hanging wall rollover can be found which dips south toward the fault scarp by as much as 10–20° (±5°). Below we describe how values for the combined vertical offset (that is, taken from the hangingwall surface, and summing the vertical dimensions of anticlinal buckles, the monocline and the fault scarp, see Fig. 4c), compare with values for the map width of the monoclines.

The monocline width in map view increases from a minima at the overall tips of the White Rabbit Fault, to values of around 45 m at c. 1100 m along the overall fault trace (Fig. 8a and d). The values appear to increase systematically from the tips of the fault towards the centre of its map trace, consistent with the hypothesis that it is a single structure as seen from the air photo (Fig. 1e). However, in contrast, a plot of the total vertical offset versus distance along the White Rabbit Fault (Fig. 8c) shows considerable fluctuation along strike. A maximum vertical offset of ~8 m is located near the centre of fault trace, with values decreasing to zero towards the lateral tips, but variability in vertical offsets occur where relay ramps exist along the fault trace. The arrows on Fig. 8c show that the locations of relay ramps coincide with minima in total vertical offset.

We interpret the fluctuations as being due to remnant displacement minima between originally soft-linked precursor fault segments that have now been breached by ongoing displacements. In particular, we note that vertical offset values decrease to close to zero at c.1500 m along the fault strike (Fig. 8c). This appears to be evidence that 2 fault segments have linked at around 1500 m along the trace of the overall fault, and that little displacement has accumulated at this point since linkage.

If we assume that the rate of displacement accumulation has remained constant through time at any given point along the fault trace, the ratio of displacement on the through-going fault to the displacement across the breached relay that accumulated prior to breaching gives an estimate of when in the displacement history breaching events occurred (Cartwright et al., 1995). We have calculated breaching index values for all the relay zones we identified along the White Rabbit Fault, and values range between 90 and 5%. This suggests that breaching of relays occurred diachronously along the fault. For example the relay ramp at c. 900 m along the fault trace breached when there was still c. 85% of the total displacement to accrue. In contrast, the relay ramp at c. 1500 m along the fault trace breached more recently, when there was only c. 5% of the total displacement at that point left to accrue. Importantly for our discussion of fault growth below, the width of the monocline in map view does not show a minimum at 1500 m along strike, even though this relay ramp breached after 95% of the displacement accumulation (compare Fig. 8c, d and e), or minima associated with the other relay-ramps. At 1500 m along the fault trace the monocline, although subdued in terms of vertical offset, is clear on the ground and air photos, and has width of c. 25 m. Below we discuss why a clear vertical displacement minima exists at c. 1500 m along the strike of the White Rabbit Fault, with very recent breaching of a relay ramp, whilst the width of the monocline does not show a minima at this point.

6. Discussion

Our most important finding is that monocline width varies systematically and relatively smoothly with distance from the fault tips towards the centre of the fault map trace (Fig. 8d), whereas total vertical offset exhibits minima close to relay-ramps superimposed on the overall trend where vertical offsets are greatest close to the centre of the fault trace (Fig. 8c). If we sample vertical offsets away from relay-ramps (see Fig. 8c), and plot them against

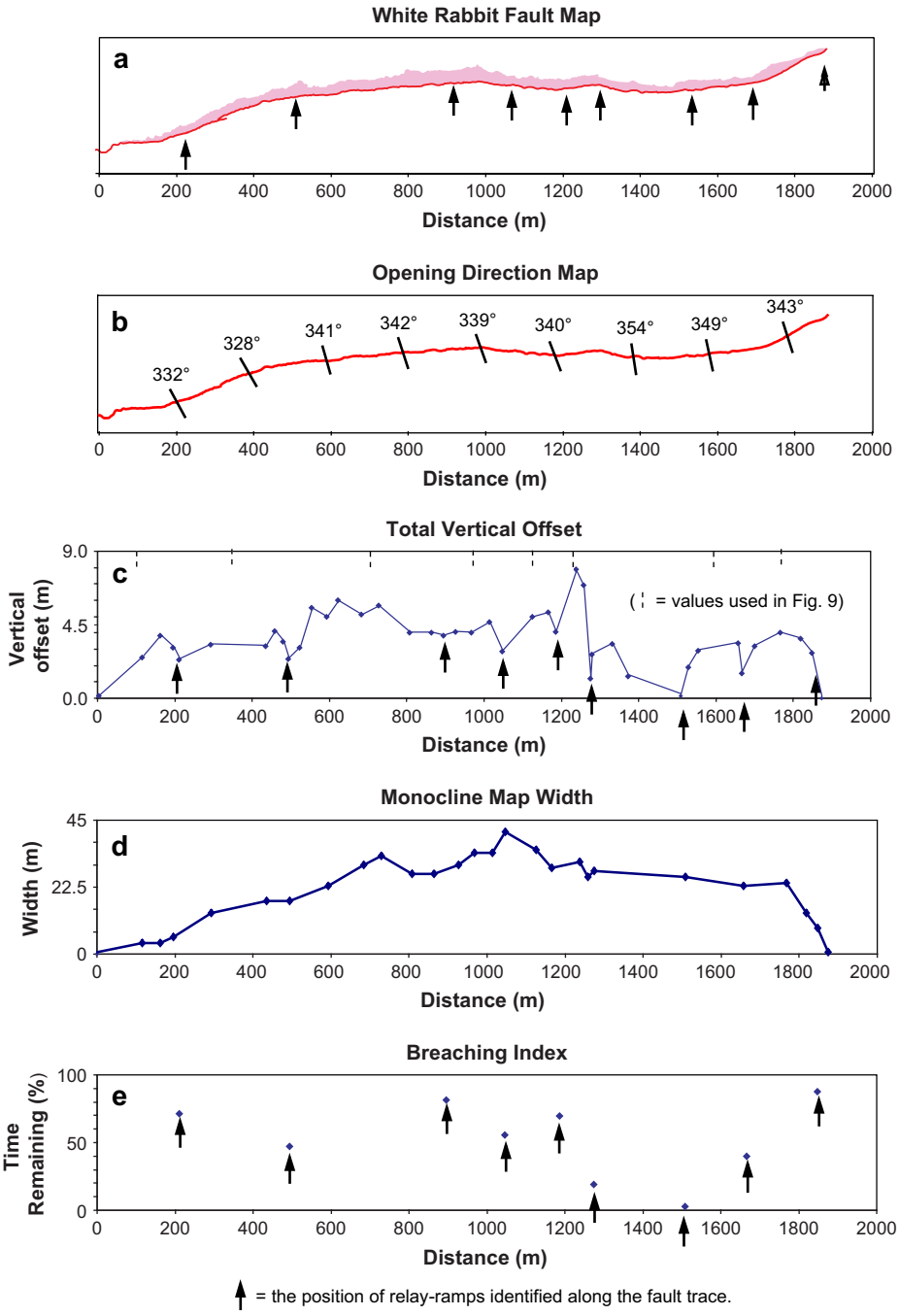

Fig. 8. (a) Trace of White Rabbit Fault (solid line) and flanking monocline (shaded). (b) Diagram indicating mean opening direction at 200 m intervals along strike of fault. (c) Plot of monocline height plus scarp height relative to distance (see Fig. 4c for explanation of how the measurements were made); note the minima at relay ramps. Dashed vertical lines show where the vertical offsets and monocline widths were sampled for Fig. 9. (d) Plot of monocline width relative to distance; note the single maxima. (e) Plot of breaching index for breached relay zones. The index gives an indication of the relative times when fault segments joined.

monocline width, it is clear that monocline widths are greatest where vertical offsets are greatest (Fig. 9; $R^2 = 0.76$). The observations are not consistent in a simple way with the idea that monocline width decreases through time as the upper tip of the fault propagates towards the surface (cf. Martel and Langley, 2006), because the monocline widths are greatest where vertical offsets at the surface are greatest. However, we suggest an alternative hypothesis to explain the monocline width to vertical offset relationship.

We suggest the single maxima in monocline width is consistent with the hypothesis that a single fault at depth was re-surfaced by a lava flow with subsequent re-emergence through upward propagation of at least 2 apophysese of the fault surface which then linked along strike at the surface within the new lava (Fig. 10). The relay-ramps are relatively short-lived, because they form and become breached in the time period between lava-resurfacing and propagation of the fault to rejoin at the surface (<500–750 years in this case; Holcomb, 1987). The monocline forms during faulting as the pre-existing fault at depth, which may extend to depths of hundreds to thousands of metres if its down-dip extent is similar to its along strike length, forces its way back to the surface through the un-faulted lava. We suggest the width of the monocline is set by the

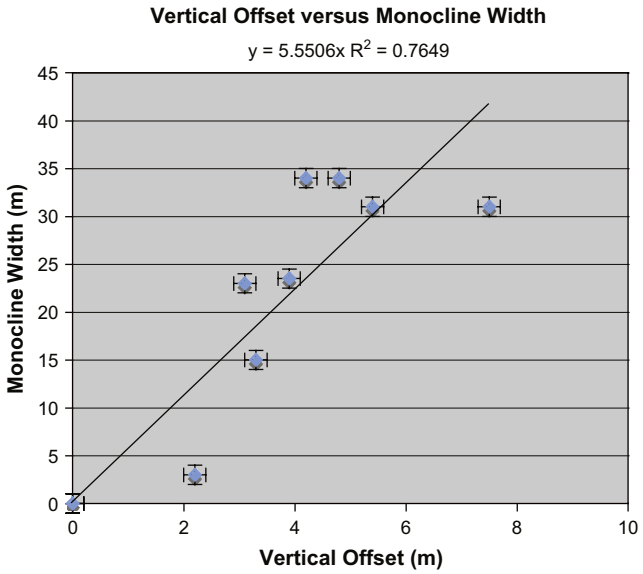

Fig. 9. Monocline width versus vertical offset.

heave of the fault at the base of the resurfacing lava (Fig. 10c). Our growth model is consistent with the observation that these north-facing scarps are known to divert and pond lava flows. This occurred most recently in 1974 from fissure eruptions in the Southwest Rift Zone (Holcomb, 1987; Fig. 1e). Our model is also consistent with the observations of Swanson et al. (1992) who descended on ropes into 15 ground cracks in the Koa'e fault system, and observed that prior lava flows have ponded against a pre-existing fault scarp at a depth of 14 m and 18.5 m.

The difference between our growth model and others (Martel and Langley, 2006; Kaven and Martel, 2007) is that we explicitly consider lava resurfacing of a pre-existing fault. We suggest that the width of the monocline will depend on the heave at the base of the new lava, rather than simply the depth of the upward propagating fault tip (although this will have an effect), because the new lava does not contain a fault when monocline growth initiates within it; thus, the hangingwall and footwall are not decoupled at the surface by a vertical fracture (Grant and Kattenhorn, 2004), and must deform over the length-scale of the decoupled surface at the base of the recent, un-faulted lava (see Fig. 10c). The material undergoing faulting is thus not a "linear elastic, isotropic, isothermal, homogeneous, semi-infinite continuum" (c.f. Martel and Langley, 2006), because at depth the lava contains pre-existing faults, whilst recent lavas at the surface are unfaulted. Although monocline dimensions and geometry may provide information on modes of vertical propagation of faults in ideal cases where accumulation of stratigraphy has not occurred during faulting (e.g. Martel and Langley, 2006; Holland et al., 2006), interpretation of propagation is more complicated if stratigraphy has accumulated during faulting (growth faulting). One must consider whether the fault was already essentially at the surface and covered by a relatively thin veneer of lava (a few metres to tens of metres; Swanson et al., 1992) when the monocline at the present surface began to grow. Fault geometries within the surface lava simply tell us about the re-emergence through upward propagation – for a few metres or tens of metres – of a pre-existing fault. Whether such small-scale upward propagation typified earlier faulting cannot be interpreted from observations of monoclines in surface lavas because both the surface lavas and the monoclines they contain had not formed during earlier fault growth. Sub-surface data on the lava thicknesses and fault heaves at depth are needed to test our hypothesis.

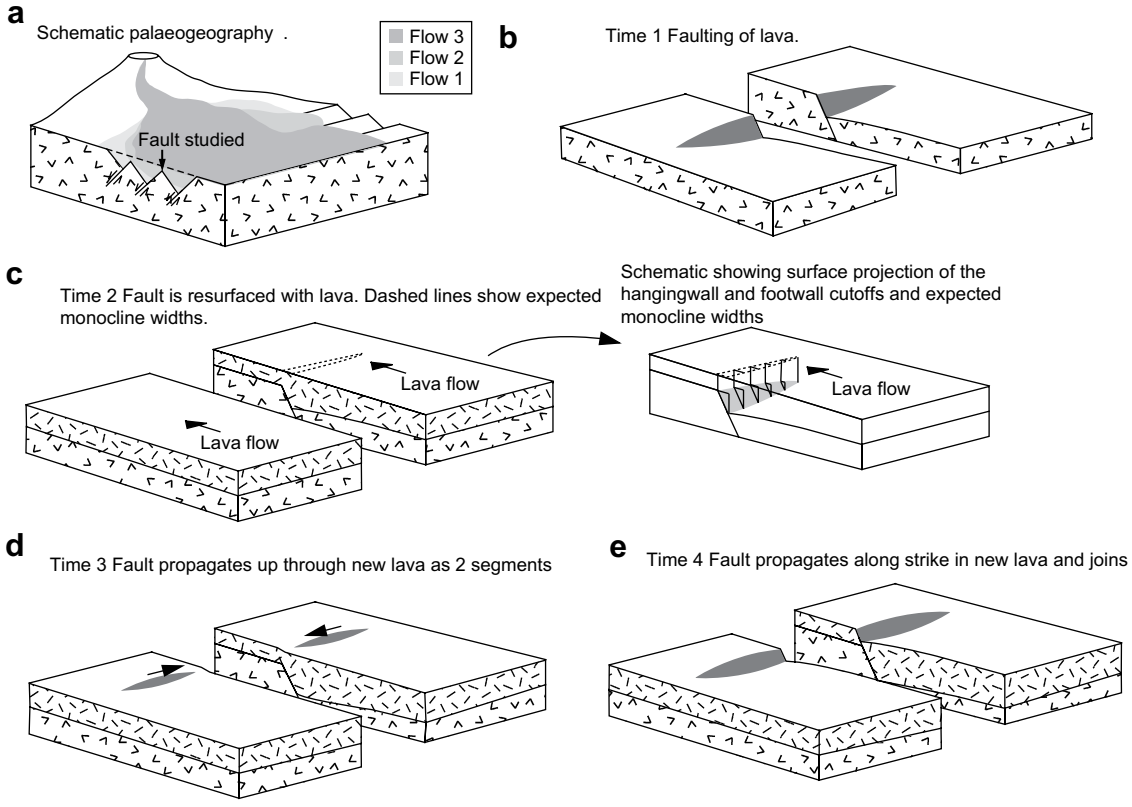

Fig. 10. Fault growth model. (a) Fault geometry relative to the volcano. (b) Time 1, a fault has produced offsets of a lava surface. (b) Time 2, the fault is re-surfaced by a lava flow that removes all trace of the fault at the surface; (c) Time 3, the fault has propagated upward to the surface as two or more segments that begin to propagate along strike towards each other. (d) Time 4, two fault segments have linked, producing a double displacement maxima.

The above implies that the Koa'e fault system has not developed since the last lava re-surfacing event, but rather, is long-lived and has throws that approach those of the Hilina fault system (Figs. 1 and 10). If we use the monocline width as a proxy for the heave and hence throw of the fault at depth beneath recent lavas (see Fig. 10c and assuming a 45° fault dip), the 1.9 km long White Rabbit Fault has a maximum throw of at least c. 40 m, not 8–9 m as suggested by offsets of the present-day ground surface (Fig. 8). The value of c. 40 m is a minimum because throws will increase with depth along a growth fault, and the c. 40 m value applies only to the base of most recent lava that was not decoupled at the surface by a vertical fracture; older layers will have greater offsets. Thus, throw and length data for the White Rabbit Fault compare with topographic offsets across the Hilina Faults (Fig. 1), because some of these latter structures have lengths of a few kilometres and topographic offsets of a few tens to hundreds of metres. The relatively subdued topographic expression of the Koa'e fault system compared to the Hilina fault system (Fig. 1), is due to lava infilling the hangingwall depressions formed by the former, as suggested by Day et al. (2005). It is implied that the rates of lava deposition are similar to the rates of vertical offset across the Koa'e fault system. We have no data that reveal the absolute age of the Koa'e fault system. However, we point out that the Hilina seaward-facing fault scarps, downslope of the Koa'e fault system (Fig. 1), expose the oldest subaerial lavas on Kilauea. One notable feature (Easton, 1987) is that the long-term lava accumulation rate in the sequences exposed around the Hilina faults decreases at around 20–30 ka. The volcanic sequence between the Middle Pohakaa Ash (43 ka) and the Pahala Ash (22.5 ka) took about 20 kyr to form, but is 3–4 times thicker than the volcanic sequence that formed since 22.5 ka. One way of explaining this is that development of the north-facing Koa'e fault system has blocked southward flow of lavas for at least some of the time since 20–30 ka, perhaps dating the first emergence of these fault scarps on a scale large enough to block lava flows. Our observations, which reveal the existence of long-lived normal faults facing uphill towards Kilauea (possibly since 20–30 ka), are consistent with the postulated uphill-facing offshore Kalapana Fault that Day et al. (2005) suggest was involved in the 1975 M7.2 Kalapana earthquake. The Koa'e fault system uphill-facing scarps will pond lavas and shield the Hilina fault system from lava sourced from the summit; this may explain why the hangingwalls to the Hilina faults have not been infilled by lavas to any great extent. Ponding of lavas high on the volcanic edifice in the hangingwall of the uphill facing scarps will influence stability of the volcanic edifice (Day et al., 2005).

7. Conclusions

We have presented observations that suggest that faults in the Koa'e fault system, Hawaii, have re-emerged via upwards propagation through lavas that have re-surfaced pre-existing faults. The upward propagating fault produces a monocline at the surface whose across strike width is controlled by the heave at depth on the pre-existing fault at the base of the most recent lava. The monocline develops because the lavas at depth in the footwall and hangingwall of the fault are decoupled across the fault whereas the most recent lava contains no fault and thus has to deform over the length-scale of the decoupling at depth, that is, the heave at depth. The monocline then becomes faulted as the pre-existing fault at depth, which may extend to depths of hundreds to thousands of metres if its down-dip extent is similar to its along strike length, forces its way back to the surface through the un-faulted lava. In the example studied herein, upward propagation involved growth of at least two separate fault segments, that are apophysese joined to a single fault at depth; the apophysese linked along strike after reaching the surface. The monocline observed at surface formed *since* deposition of the most recent lava (<500–750 years), so study of the amplitude and wavelength of such structures cannot reveal the geometry or mechanics of deformation that occurred prior to deposition of the most recent lava. The monocline cannot be used constrain upward propagation from depths greater than the thickness of the most recent lava (metres to tens of metres). The growth fault geometries that result from upward propagation through re-surfacing lavas suggest that rates of vertical motion across the faults are similar to rates of lava deposition (Day et al., 2005). The growth faults face uphill to towards the summit of the volcano and so pond lavas high on the volcanic edifice, starving the lower slopes of lava. Overall, the Koa'e faults are growth faults that pre-date the lavas exposed at the surface on the volcano flank, and are a long-lived feature of the volcano dynamics, despite the small offsets across the faults at the surface.

Acknowledgements

Funding for this project was provided in part by the 2005 University of London Dunsheath Expedition Award and the 2005 USGS Jack Kleinman Grant for Volcano Research awarded to Dean Podolsky, who would also like to acknowledge the kind and generous support of the staff at the USGS Hawaiian Volcanoes Observatory, especially Steve Brantley, Jim Kauahikaua, Rick Hoblitt, Christian Heliker, Taeko Jane Takahashi and Paul Okubo. Special thanks go to Don Swanson and Tim Orr of HVO whose support and generous time benefited us enormously. Discussions with David Peacock, Simon Day and John Cosgrove improved our understanding of the volcano and its faults. Simon Day pointed out the stratigraphic data that support our interpretation. Access to the study area was made possible by Tim Tunison and National Park Permit #HAVO-2004-SCI-0035 (Study #HAVO-00129). We thank anonymous referees for their comments.

References

Cartwright, J.A., Mansfield, C.S., 1998. Lateral displacement variation and lateral tip geometry of normal faults in the Canyonlands National Park, Utah. Journal of Structural Geology 20, 3–19.

Cartwright, J.A., Trudgill, B.D., Mansfield, C.S., 1995. Fault growth by segment linkage: and explanation for scatter in maximum displacement and trace length data from the Canyonlands Grabens of SE Utah. Journal of Structural Geology 17, 1319–1326.

Clague, D.A., Dalrymple, G.B., 1987. The Hawaiian-Emperor Volcanic Chain. In: Professional Paper 1350. United States Geological Survey. 5–54.

Day, S.J., Watts, P., Grilli, S.T., Kirby, J.T., 2005. Mechanical models of the 1975 Kalapana, Hawaii earthquake and tsunami. Marine Geology 215, 59–92.

Duffield, W.A., 1975. Structure and Origin of the Koae Fault System, Kilauea Volcano, Hawaii. In: Professional Paper 856. United States Geological Survey.

Easton, R.M., 1987. Stratigraphy of Kilauea volcano. In: Decker, R.W., Wright, T.L., Stauffer, P.H. (Eds.), Volcanism in Hawaii. Professional Paper 1350. United States Geological Survey, pp. 243–260.

Fiske, R.S., Koyanagi, R.Y., 1968. The December 1965 Eruption of Kilauea Volcano, Hawaii. In: Professional Paper 607. United States Geological Survey.

Grant, J.V., Kattenhorn, S.A., 2004. Evolution of vertical faults at an extensional plate boundary, southwest Iceland. Journal of Structural Geology 26, 537–557.

Holcomb, R.T., 1987. Eruptive History and Long Term Behavior of Kilauea Volcano. In: Professional Paper 1350. United States Geological Survey. 261–351.

Holland, M., Urai, J.L., Martel, S., 2006. The internal structure of fault zones in basaltic sequences. Earth and Planetary Science Letters 248, 286–300.

Kaven, J.O., Martel, S.J., 2007. Growth of surface-breaching normal faults as a three-dimensional fracturing process. Journal of Structural Geology 29, 1463–1476.

Kinoshita, W.T., 1967. May 1963 earthquakes and deformation in the Koae Fault Zone, Kilauea Volcano Hawaii. In: Professional Paper 575-C. United States Geological Survey. C173–C176.

Koyanagi, R.Y., Swanson, D.A., Endo, E.T., 1972. Distribution of earthquakes related to mobility of the south flank of Kilauea Volcano, Hawaii. In: Professional Paper 800-D. United States Geological Survey. D89–D97.

Macdonald, G.A., 1957. Faults and monoclines on Kilauea Volcano, Hawaii. Bulletin of the Geological Society of America 68, 269–271.

Martel, S.J., Langley, J.S., 2006. Propagation of normal faults to the surface in basalt, Koae fault system, Hawaii. Journal of Structural Geology 28, 2123–2143.

McGill, G.E., Stromquist, A.W., 1975. Origin of grabens in the Needles district, Canyonlands National Park, Utah. Four Corners Geological Society, Durango, CO. 235–243.

McGill, G.E., Stromquist, A.W., 1979. The grabens of Canyonland National Park, Utah: geometry, mechanics, and kinematics. Journal of Geophysical Research 84, 4547–4563.
Peacock, D.C.P., Parfitt, E.A., 2002. Active relay ramps and normal fault propagation on Kilauea Volcano, Hawaii. Journal of Structural Geology 24, 729–742.
Parfitt, E.A., Peacock, D.C.P., 2001. Faulting in the South Flank of Kilauea Volcano, Hawaii. Journal of Volcanology and Geothermal Research 106, 265–284.
Stromquist, A.W., 1976. Geometry and growth of grabens, Lower Red Lake Canyon area, Canyonlands National Park, Utah. Contribution No. 28. Department of Geology and Geography, University of Massachusetts, Amherst, MA, 118 pp.
Swanson, D.A., Duffield, W.A., Fiske, R.S., 1976. Displacement of the south flank of Kilauea Volcano: the result of forceful intrusion of magma into the rift zone. In: Professional Paper 963. United States Geological Survey.
Swanson, D.A., Fiske, R.S., Rose, T.R., 1992. Recurrent faulting in Kilauea's breakaway rift system indicated by ponded lava flows in the Koa'e Fault System. In 1992 Fall Meeting, American Geophysical Union, supplement to Eos, Transactions of the American Geophysical Union.